Project acronym:	**Geo-Drill**
Project title:	Development of novel and Cost-Effective drilling technology for geothermal Systems
Activity:	LCE-07-17-Renewables
Call:	H2020-LC-SC3-2018-RES-TwoStages
Funding Scheme:	RIA	**Grant Agreement No:**	815319
WP7	**Simulation, KBS and DSS**

D7.2 Report on Drill String Physics Simulator

Due date:	30/09/2021 (M28)	
Actual Submission Date:	28/10/2021	
Lead Beneficiary:	FPS	
Main authors/contributors:	FPS	
Dissemination Level[1]:	PU	
Nature:	Report	
Status of this version:		**Draft under Development**
		For Review by Coordinator
	X	**Submitted**
Version:	02	

REVISION HISTORY

Version	Date	Main Authors/Contributors	Description of changes
v01	30.09.2021	FPS	First version
V02	20.10.2021	FPS	Added more details + examples

Funded by the Horizon 2020 Framework Programme of the European Union

1 Dissemination level security:

PU – Public (e.g. on website, for publication etc.) / **PP** – Restricted to other programme participants (incl. Commission services) / **RE** – Restricted to a group specified by the consortium (incl. Commission services) / **CO** – confidential, only for members of the consortium (incl. Commission services)

This project has received funding from the European Union's Horizon 2020 program Grant Agreement No 815319. This publication reflects the views only of the author(s), and the Commission cannot be held responsible for any use which may be made of the information contained therein.

Document: D7.2 Report on Drill String Physics Simulator

Version: 2

Date: 27/10/21

Summary

A new powerful engineering analyses software for geothermal flow assurance is under development by Flowphys AS. This software is capable of simulating single-phase and multi-phase dynamic (time-dependent) flows in complex pipe networks and is based on conservation equations. Part of the software development is carried out in several H2020 projects: GeoCoat, GeoSmart, GeoPro, GeoDrill, and Eurostars ProCase.

In this report, a new Finite Element Method (FEM) solver for structural static and dynamic analyses has been developed. This solver has been combined with the Flow Assurance Simulator software to enable multi-physics (structural dynamics, fluid dynamics, thermodynamics, and heat transfer) simulations of drilling operations. The combination forms a Drill String Physics Simulator, which is also the fundament for the Drill Monitor that is to be developed in Task T7.3, which in addition to the simulator also takes sensor readings into account.

CONTENTS

1. INTRODUCTION

To simulate drilling operations requires multi-physics simulations, as it includes fluid flow, heat transfer, and structural dynamics. In Geo-Drill delivery report D7.1 "Geothermal Well Flow Assurance Simulator" [1], the fundamentals of the Flowphys Geothermal Flow Assurance simulator software are provided. This simulator is capable of analyzing the fluid flow, thermodynamics, and heat transfer in wells as well as other parts of a geothermal powerplant. To summarize, it contains the following main features:

- FEM-based fluids and heat transfer solver for flows in general pipe networks
- Steady state and transient multi-phase, multi-component flows
- Several different options for fluid properties, including non-Newtonian fluids (e.g. for drilling mud), geochemical calculations through PHREEQC [2], and silica reaction kinetics.
- Device models such as pumps, valves, wells, heat exchangers, fans, turbines, separators, etc
- Annulus flows
- GUI specialized for the geothermal energy market, also including a drilling module

The current report outlines a new structural Finite Element Method (FEM) solver that has been developed and added into the Flowphys Geothermal Flow Assurance software suite. This new structural FEM software contains a generalized 1D element that combines bending, tension, and torsion, with 6 DOFs (Degree-of-Freedom) at each node. Both static and dynamic simulations can be carried out.

2. STRUCTURAL STATICS FEM SOLVER

2.1 FUNDAMENTALS

A new finite element method solver for structural static and dynamic analyses has been developed and implemented into the Flowphys software. The spatial discretization is a generalized 1D element in 3D space, i.e. a combination of an Euler-Bernoulli beam element, rod element for tension, and a rod element for torsion. The element has 2 nodes and 6 DOFs at each node, resulting in elemental 12x12 stiffness matrices. The stiffness matrix is solved by a pre-conditioned Conjugate Gradient matrix solver. The whole software, including the matrix solver, is coded in Fortran and has been developed by Flowphys (FPS).

2.2 STATIC ANALYSIS EXAMPLES

To validate the new FEM solver, several test examples have been carried out. In Figure 2.1, static deflection of a cantilever beam with distributed load have been calculated with the FEM solver using 5 elements and 20 elements. The computational results are compared with the exact solution using Euler-Bernoulli theory of slender beams [3],

$$\Delta y = \frac{QL^3}{24EI}\left(\left(\frac{L-x}{L}\right)^4 - 4\left(\frac{L-x}{L}\right) + 3\right) \tag{2.1}$$

where Q is the distributed load, L is the length of the beam, E is the Young's modulus, and I is the area moment of inertia. For this test case, Q=ρALg, ρ=7800 kg/m^3, E=210 GPa, and L=5 m. The beam cross-section is a thick-walled pipe (similar to a drilling pipe), with inner diameter h_inner=60mm, and outer diameter h_outer=100 mm. Two meshes were used, one with 5 and the other with 20 finite elements.

As expected, from Figure 2.1 it is seen that the FEM results with 20 elements is closer to the exact solution (from Eq. 2.1) than the case with only 5 finite elements.

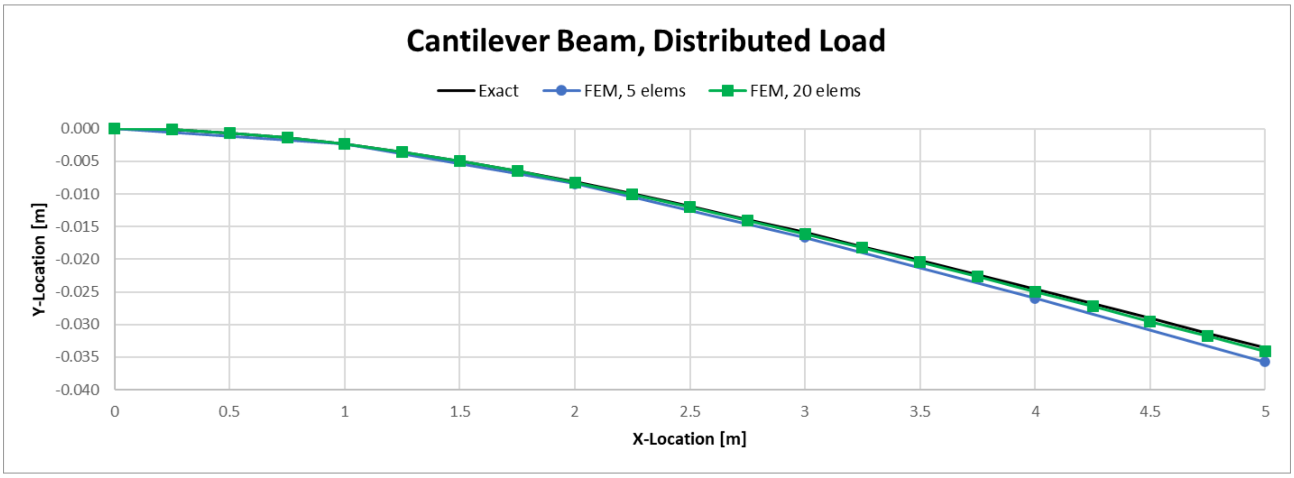

Figure 2.1: Results with the newly developed FEM solver using 5 and 20 finite elements, compared with the exact solution for slender beams. Notice that X- and Y-axes have different scales.

Similarly to bending, analyses for longitudinal and torsional DoFs were performed, with point loads or point moments applied at the end of the cantilever beam. For axial or longitudinal analyses, the displacement can be calculated as

$$\Delta\mathrm{x} = \frac{PL}{EA} \tag{2.2}$$

where P is the point load and A is the cross-section area. The results for the longitudinal calculations are in agreement with the exact solution as is shown in Table 2.1.

Table 2.1: Comparison calculations and exact solution for longitudinal DoF

Load [kN]	Δx Calc [m]	Δx Exact [m]
200	0.00094735	0.00094735
1000	0.0047368	0.0047368

For torsion, the exact angle of twist can be calculated as

$$\Delta\theta = \frac{ML}{GK} \tag{2.3}$$

where G is the shear modulus, K is the polar moment of inertia, and M is the moment applied at the end of the cantilever beam. The FEM torsional calculations are shown in Table 2.2 and are in good agreement with the exact results.

Table 2.2: Comparison calculations and exact solution for torsional DoF

Load [Nm]	Δθ Calc [rad]	Δθ Exact [rad]
20000	0.14489	0.14489
100000	0.72444	0.72444

3. STRUCTURAL DYNAMICS FEM SOLVER

3.1 GOVERNING EQUATIONS AND FEM MATRICES

For structural dynamics, the equation of motion is

$$\mathrm{m}\ddot{\mathrm{d}} + \mathrm{c}\dot{\mathrm{d}} + \mathrm{kd} = \mathrm{f} \tag{3.1}$$

where d is the displacement vector, f is the (external) force vector, m is the mass matrix, c is the damping matrix, and k is the same stiffness matrix as for the static solver described in Section 2. Just like the stiffness matrix, the mass and damping matrices also have elemental 12x12 matrices.

The damping matrix c is calculated as Rayleigh damping, where the damping matrix is a combination of the stiffness and mass matrices,

$$\mathrm{c} = \mu\mathrm{k} + \lambda\mathrm{m} \tag{3.2}$$

where μ and λ are (scalar) coefficients. The damping will vary depending on frequency. For structural dynamics that use modal superposition, it is possible to set the damping for each eigen mode. However, for direct time integration, which is the method used here, the values of μ and λ are chosen by setting the values of the damping at two different frequencies that span the design spectra. The damping matrix coefficients are then calculated as [4],

$$\mu = \frac{2(\xi_H\omega_H - \xi_L\omega_L)}{\omega_H^2 - \omega_L^2} \tag{13}$$

$$\lambda = \frac{2\omega_L\omega_H(\xi_L\omega_H - \xi_H\omega_L)}{\omega_H^2 - \omega_L^2} \tag{24}$$

where ξ_L is the fraction of critical damping at the low end of the design spectra and ξ_H is the fraction of critical damping at the high end. The design spectra would typically cover frequencies from the lowest frequency of interest, i.e. the 1st eigenfrequency, to the highest frequency of interest. The latter depends on if it is an impact problem such that high frequencies are excited, or a non-impact vibration problem in which case the first few eigenfrequencies are sufficient for a good description of the dynamics.

For a general structure, it is in general a good idea to always first perform a modal analysis to check that all eigenmodes of interest are properly resolved with the mesh, and also to provide input for the frequency spectra of interest in the analyses, such that for example the Rayleigh damping coefficients can be calculated.

For the cases shown here, torsion and tension rods, the eigenfrequencies can be calculated exactly from [5],

$$\text{Torsional eigenfrequencies: } f_n = \frac{2n-1}{4L}\sqrt{\frac{G}{\rho}} \tag{35}$$

$$\text{Longitudinal eigenfrequencies: } f_n = \frac{2n-1}{4L}\sqrt{\frac{E}{\rho}} \tag{46}$$

where f_n is eigenfrequency of the n:th eigenmode. For a cantilever beam, the 3 first transversal eigenfrequencies are [5]

$$\text{1st bending eigenfrequency: } f_1 = \frac{3.52}{2\pi}\sqrt{\frac{EI}{\rho A L^4}} \tag{57}$$

$$\text{2nd bending eigenfrequency: } f_1 = \frac{22.0}{2\pi}\sqrt{\frac{EI}{\rho A L^4}} \tag{68}$$

$$\text{3rd bending eigenfrequency: } f_1 = \frac{61.7}{2\pi}\sqrt{\frac{EI}{\rho A L^4}} \tag{79}$$

3.2 TIME DISCRETIZATION

An implicit Newmark method [4] has been implemented for the time stepping. Notice that this is the same method as used for the rigid body oscillation in Geo-Drill D4.3 report [6]. The Newmark method used here is an unconditionally stable method, i.e. in theory it is stable for any size of the timestep. However, the timestep still of course needs to be small enough to provide sufficient accuracy or capture higher frequencies such as for example generated at impacts.

With the Newmark method, the structural dynamics equations to be solved are

$$\begin{aligned}
&\left[\frac{1}{\alpha\Delta t^2}\mathrm{m} + \frac{\delta}{\alpha\Delta t}\mathrm{c} + \mathrm{k}\right]\mathrm{d}_{n+1} = \mathrm{f}_f \\
&+ \mathrm{m}\left[\tfrac{1}{\alpha\Delta t^2}\mathrm{d}_n + \tfrac{1}{\alpha\Delta t}\dot{\mathrm{d}}_n + \left(\tfrac{1}{2\alpha} - 1\right)\ddot{\mathrm{d}}_n\right] \\
&+ \mathrm{c}\left[\frac{\delta}{\alpha\Delta t}\mathrm{d}_n + \left(\frac{\delta}{\alpha} - 1\right)\dot{\mathrm{d}}_n + \frac{\Delta t}{2}\left(\frac{\delta}{\alpha} - 2\right)\ddot{\mathrm{d}}_n\right]
\end{aligned} \tag{810}$$

where

$$\ddot{\mathrm{d}}_{n+1} = \frac{1}{\alpha\Delta t^2}[\mathrm{d}_{n+1} - \mathrm{d}_n] - \frac{1}{\alpha\Delta t}\dot{\mathrm{d}}_n - \left(\frac{1}{2\alpha} - 1\right)\ddot{\mathrm{d}}_n \tag{911}$$

$$\dot{\mathrm{d}}_{n+1} = \dot{\mathrm{d}}_n + \Delta t(1-\delta)\ddot{\mathrm{d}}_n + \delta\Delta t\ddot{\mathrm{d}}_{n+1} \tag{3.12}$$

$$\alpha = \frac{1}{4}(1+\gamma)^2 \tag{1013}$$

$$\delta = \frac{1}{2} + \gamma \tag{1114}$$

Here, γ is the amplitude decay factor, which is set to γ=0.005 to reduce numerical spurious oscillations. This also reduces the time stepping from a second order to a first order accurate algorithm. However, as the decay factor is small, the second-order error term is also very small, making it almost second order accurate in time.

3.3 DYNAMIC ANALYSIS EXAMPLES

The same thick-walled pipe as used in the static analysis examples in Section 2 is used for the dynamic analysis examples in this section.

3.3.1 Longitudinal vibration

In this example, an axial load is applied on the free end of the cantilever beam. The magnitude of the axial load is 1000 kN in the time interval 0.01-0.11 s, and zero otherwise. To determine suitable timestep and Rayleigh damping parameters, we first need to have an idea about relevant eigenfrequencies. From Equation (3.6), the 1st longitudinal eigenfrequency is calculated to

$$f_1 = \frac{1}{4L}\sqrt{\frac{E}{\rho}} = 259\ Hz \tag{1215}$$

Thus, the period is T_1=3.85ms. Using Eq. (2.6), it can be seen that the 3rd eigenfrequency is 1300 Hz. To enable good resolution of the first eigenmode and acceptable also for the 3rd, a timestep of Δt=0.1ms is chosen. For calculating the Rayleigh damping parameters, f_L=259 Hz and f_H=1300 Hz were used, and 0.4% fraction of critical damping was assumed. Calculation was performed with the Newmark method. The time-history of the longitudinal displacement of the free end of the cantilever beam is shown in Figure 3.1. A zoom-in of the results is shown in Figure 3.2. From this figure, it is possible to estimate the vibration frequency to f_1 ≈257 Hz, close to the theoretical value of 259 Hz given above. Moreover, the displacement after the oscillations have disappeared, Δx=4.74mm, agrees with the static results in Table 2.1.

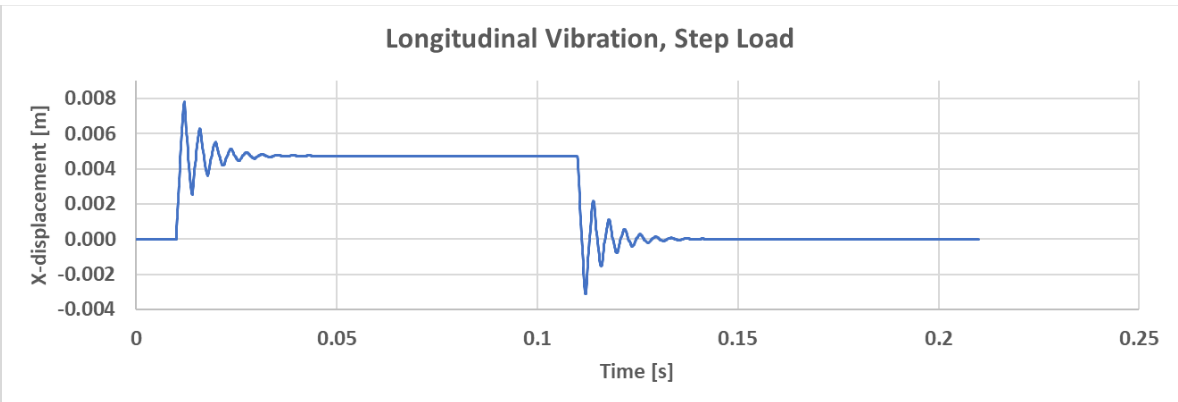

Figure 3.1: Results with the newly developed FEM structural dynamics solver using 20 finite elements. Time-history of free end of cantilever beam subjected to a longitudinal step load.

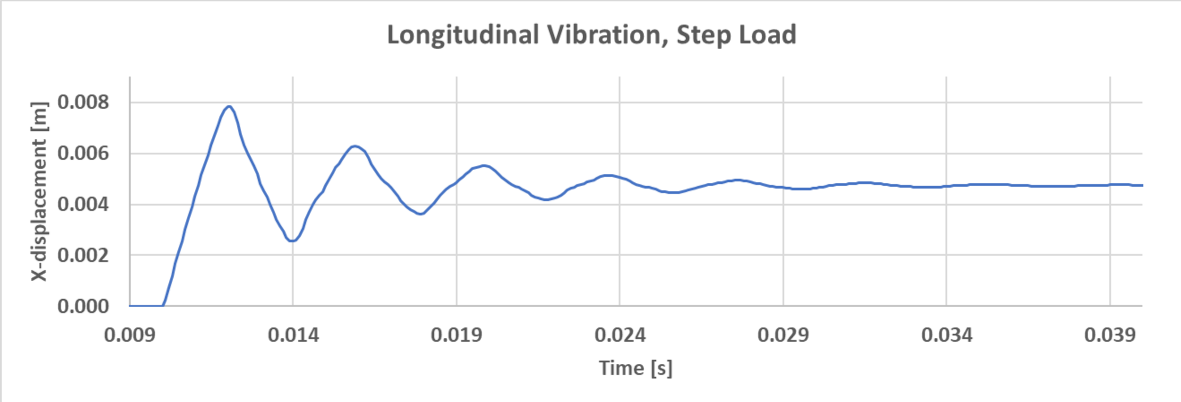

Figure 3.2: Zoom-in of time history results.

3.3.2 Transversal vibration

In this example, a transversal load is applied on the free end of the cantilever beam. The magnitude of the axial load is 1000 N in the time interval 1.0-11 s, and zero otherwise. From Equation (2.7), the 1st longitudinal eigenfrequency is calculated from

$$f_1 = \frac{3.52}{2\pi}\sqrt{\frac{EI}{\rho A L^4}} = 3.39\ Hz \tag{1316}$$

Thus, the period is T_1=0.295 s and a timestep of Δt=0.01s was chosen. For calculating the Rayleigh damping parameters, f_L=3.39 Hz and f_H=59.4 Hz were used and a 0.4% fraction of critical damping was assumed. Calculation was performed with the Newmark method. The time-history of the transversal displacement of the free end of the cantilever beam is shown in Figure 3.3. A zoom-in of the results is shown in Figure 3.4. From this figure, it is possible to estimate the vibration frequency to $f_1 \approx$3.39 Hz, which is in agreement with the theoretical prediction in Eq. (3.16). The Y-displacement after the oscillations have disappeared is Δy=46.4 mm, which agrees with the static deflection,

$$\Delta y = \frac{PL^3}{3EI} = 0.0464\ m \tag{3.17}$$

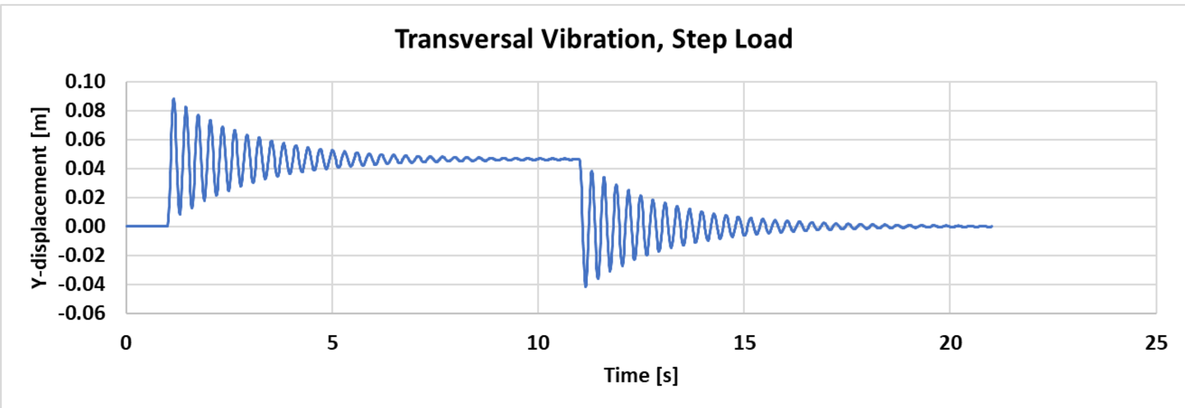

Figure 3.3: Results with the newly developed FEM structural dynamics solver using 20 finite elements. Time-history of free end of cantilever beam subjected to a transversal step load.

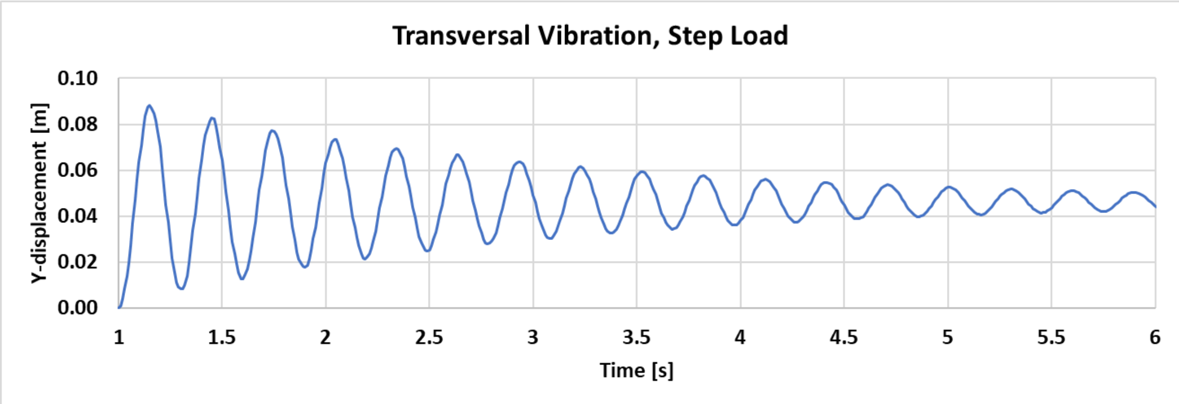

Figure 3.4: Zoom-in of time history results.

4. FLUID-STRUCTURE INTERACTION

A structure that is moving in a fluid and/or with fluid moving around the structure is subjected to fluid forces. As these forces may cause deformation or movement of the structure, which in turn may again change the fluid forces, it is in general a two-way coupled fluid-structure interaction problem. The Flowphys software is able to handle two-way coupled fluid-structure interaction using an Arbitrary Lagrangian-Eulerian (ALE) method as described in Kjellgren & Hyvarinen [7] and in report D4.3. However, to perform such computations are time-consuming and not practical for analysis of a whole drill string that might be several km long, especially not for drill monitoring purposes, where real-time simulation capability is important. Therefore, we use a simplification, where a structural dynamics system is solved, and where the fluid forces are taken into account through added mass and added damping in the structural dynamics equations of motion. The added mass and added damping are calculated beforehand through a true two-way coupled ALE fluid-structure interaction. With this approach, it is possible to take into account the fluid-structure interaction and still allow for very fast calculations.

4.1 ADDED MASS & ADDED DAMPING

Bending motions of the drill string inside the bore hole will cause transversal fluid forces on the drill string. The magnitude of these forces is dependent on the ratio between the outer diameter of the drill string h, diameter of the borehole D, vibration frequency, fluid density, and fluid viscosity. Approximating the added mass as the mass of the fluid displaced by the body is common. However, it should be noted that such an approximation is strictly only valid for infinitely long circular cylinders vibrating in a quiescent fluid without boundaries (e.g. infinitely large diameter bore hole). This common approximation is not valid for other cases with non-circular cross-sections and especially not valid when the ratio between the bore hole diameter and drill string diameter is small, i.e. the annulus is thin. This is because the fluid velocities become higher due to squeeze effects, resulting in significantly larger added mass and added damping.

For a general case, the added mass and added damping can be calculated by the method given in Kjellgren & Hyvarinen [7]. Here, the equation of motion for a body in a fluid can be expressed as

$$m\ddot{d} + c\dot{d} + kd = f_{ext} - f_f \tag{4.1}$$

where f_{ext} is an external force and f_f is the (exact) fluid force. Approximating the fluid force as added mass and added damping gives

$$f_f \approx f_{fad} = m_{ad}\ddot{d} + c_{ad}\dot{d} \tag{4.2}$$

where m_{ad} is the added mass and c_{ad} is the added damping. With this approximation, the equation of motion becomes

$$(m + m_{ad})\ddot{d} + (c + c_{ad})\dot{d} + kd = f_{ext} \tag{4.3}$$

Assuming a prescribed transversal sinusoidal motion,

$$d = A\sin\omega t \tag{4.4}$$

and expressing the fluid force acting on the body as a Fourier series gives

$$f_f = a_0 + \sum_{n=1}^{\infty} a_n\cos(n\omega t) + \sum_{n=1}^{\infty} b_n\sin(n\omega t) \tag{4.5}$$

where

$$a_0 = \frac{1}{2\pi}\int_0^{2\pi} f_f\,dt \tag{4.6}$$

$$a_n = \frac{1}{\pi}\int_0^{2\pi} f_f\cos(n\omega t)\,dt, \qquad n = 1, \dots, \infty \tag{4.7}$$

$$b_n = \frac{1}{\pi}\int_0^{2\pi} f_f\sin(n\omega t)\,dt, \qquad n = 1, \dots, \infty \tag{4.8}$$

The approximation $f_f \approx f_{fad}$ results in

$$-m_{ad}A\,\omega^2\sin\omega t + c_{ad}A\omega\cos\omega t = a_0 + \sum_{n=1}^{\infty} a_n\cos(n\omega t) + \sum_{n=1}^{\infty} b_n\sin(n\omega t) \tag{4.9}$$

Thus, the approximation by using added mass and added damping can be seen as using only the first cosinus and sinus terms of a Fourier series of the fluid force, with values

$$m_{ad} = -\frac{b_1}{A\omega^2} \tag{4.10}$$

$$c_{ad} = \frac{a_1}{A\omega} \tag{4.11}$$

By measuring the fluid forces or calculating them with CFD, it is with this method possible to calculate the added mass and added damping for arbitrarily shaped bodies.

The effects of ratio between drill string outer diameter h and bore hole diameter D has been analyzed in [7] using the Flowphys ALE functionality and comparing with analytical results derived by Chen [8]. The added mass and added damping for two different frequency Reynolds' numbers are plotted in the figures below. The frequency Reynolds' number is calculated as

$$\mathrm{Re}_{\omega} = \frac{\omega h^2}{\upsilon} \tag{4.12}$$

where υ is the kinematic viscosity.

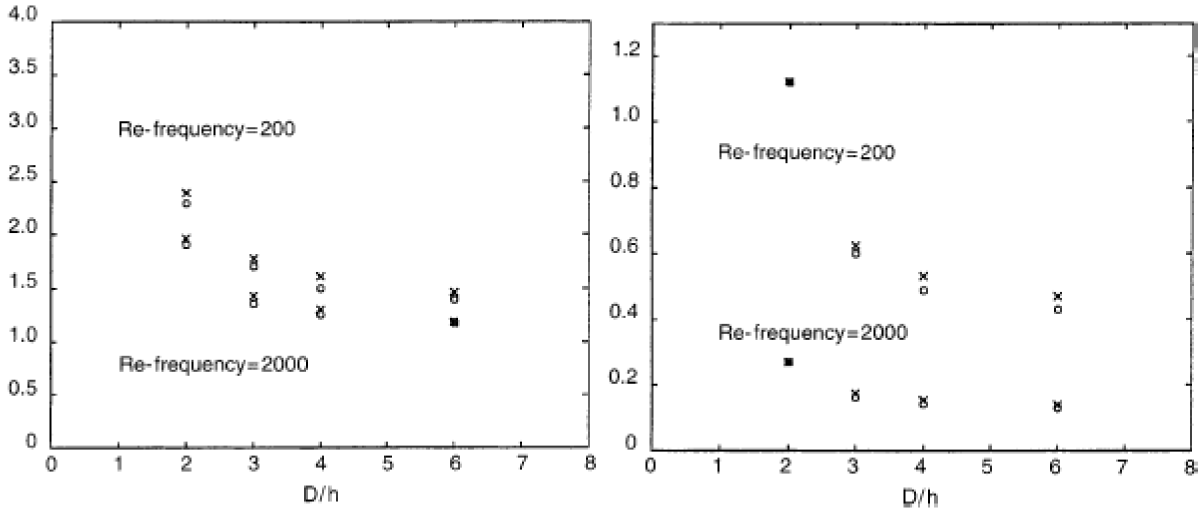

Figure 4.5: Normalized added mass $(\mathrm{m_{ad}}/(\frac{\rho\pi h^2}{4}))$ and normalized added damping $(\mathrm{c_{ad}}/(\frac{\omega\rho\pi h^2}{4}))$ versus D/h ratio for transversal vibrations of a circular cylinder in a quiescent fluid as calculated by Flowphys CFD [7] and by Chen [8]. a) Normalized added mass; b) Normalized added damping

4.2 EXAMPLE WITH ADDED MASS AND ADDED DAMPING

The transversally vibrating pipe in Section 3 does not include any surrounding fluids, i.e. it is vibrating in vacuum. It is of interest to compare this, for exactly the same pipe and force, but when it is vibrating in a fluid-filled annulus. For this, we need to add the effects of added mass and added damping. For simplicity, we assume that the kinematic viscosity for the drilling mud is υ=88e-6 m2/s, ratio of the annulus diameter D and pipe outer diameter h is D/h=2, and the density of the drilling mud is 1000 kg/m3. Thus, the frequency Reynolds' number is $\mathrm{Re}_{\omega} = 2000$ and from the graphs in Figure 4.5 we have that the added mass and damping are

$$\mathrm{m_{ad}} = 1.95\frac{\rho\pi h^2}{4} = 15.3 \text{ kg/m} \tag{4.13}$$

$$\mathrm{c_{ad}} = 0.28\frac{\omega\rho\pi h^2}{4} = 38.7 \text{ kg/sm} \tag{4.14}$$

The mass for the fluid inside the drill string also needs to be added, i.e.

$$\mathrm{m_{Inner}} = \frac{\rho\pi {h_{Inner}}^2}{4} = 2.8 \text{ kg/m} \tag{4.15}$$

The mass per length unit for the steel pipe is 39.2 kg/m. By adding the added mass from the fluid in the annulus and the fluid inside the pipe, we have the total mass=39.2 + 15.3 + 2.8=57.3 kg/m. With additional mass, the eigenfrequency will be reduced. From the theoretical calculation of the 1st transversal eigenfrequency, we have

$$f_1 = \frac{3.52}{2\pi}\sqrt{\frac{EI}{(\frac{57.3}{39.2})L^4}} = 2.80\ Hz \tag{1416}$$

Calculation was performed with the added mass and damping. The time-history of the transversal displacement of the free end of the cantilever beam is shown in Figure 4.1, where the case labeled "Quiescent fluid" corresponds to the case with added mass and added damping. Notice how the oscillation period is larger, a result of the higher mass. Notice also how the higher damping reduces the oscillation amplitude. A zoom-in of the results is shown in Figure 4.2. From this figure, it is possible to estimate the vibration frequency to $f_1 \approx 2.79$ Hz, which agrees with the theoretical prediction above. The Y-displacement after the oscillations have disappeared is Δy=46.4 mm, which agrees with the static deflection as well as the dynamic case without added mass or damping, as these do not affect the steady-state solution, only the dynamics.

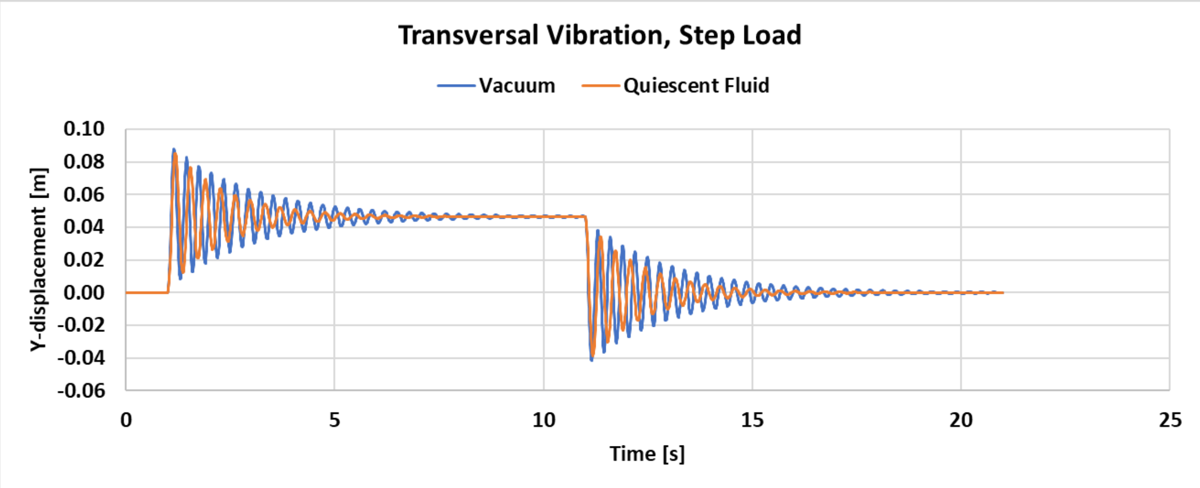

Figure 4.1: Time-history of free end of cantilever beam subjected to a transversal step load. Comparison of vibration in vacuum and in a quiescent fluid (=added mass and added damping included).

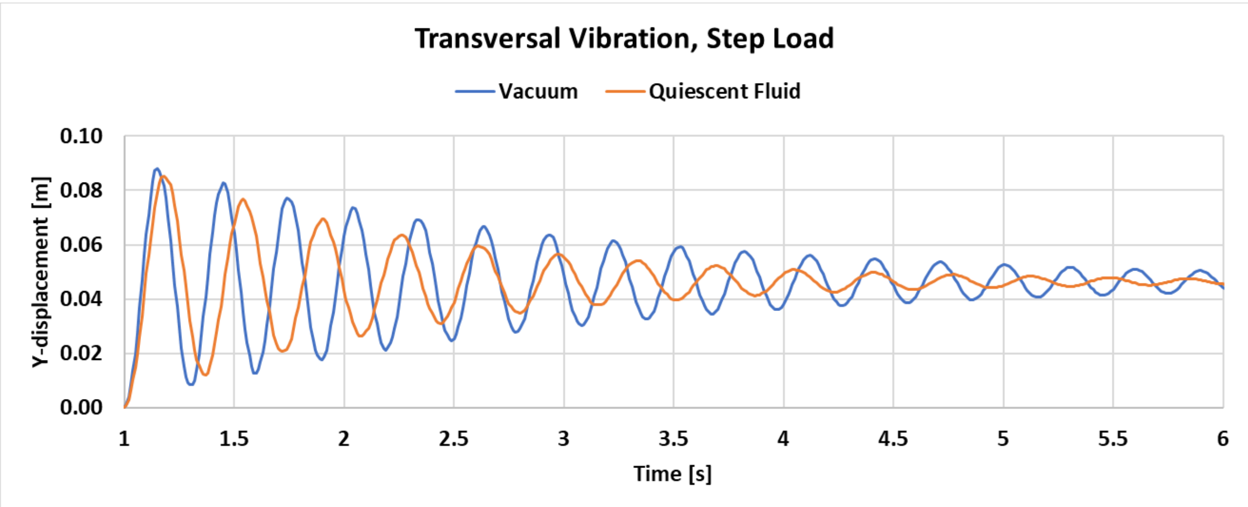

Figure 4.2: Zoom-in of time history results.

4.3 LONGITUDINAL FORCES

Similarly to the transversal forces, the added mass and added damping approach can also be used to approximate the oscillating longitudinal fluid forces caused by longitudinal vibrations of the drill string. However, it is necessary to include geometries that protrude from the drill string, such as collars etc., to calculate the forces correctly. This can be done by CFD analyses but has not been done yet, partly because the shape and dimensions of these geometries are not finalized. Moreover, the longitudinal oscillatory forces will be far larger at the bottom hole assembly than at the topside. This can be seen by looking at the amplitude of the velocity of the drill bit. For example, assuming that the hammer stroke is 0.04 m and has a frequency of 40 Hz, results in a velocity amplitude of

$$V_{\text{Amplitude}} = A\omega = 10 \text{ m/s} \tag{4.17}$$

i.e. comparable or even exceeding the velocities inside the drill string or in the annulus. In addition, there will be squeeze effects at the bottom. However, for long drill strings with many joints, the oscillation amplitude of the drill string is gradually reduced along the drill string, and approaches zero at the topside. Thus, even if the protruding geometries are the same along the drill string, the added mass and added damping would vary along the drill string, being largest at the bottom and close to zero at the top.

The static component of the shear stresses, assuming no protruding geometries, is calculated by the flow assurance simulator from the Darcy-Weisbach friction factor, both for the inside of the drill string as well as the outside in the annulus.

5. CONCLUDING REMARKS

A new FEM solver for structural static and dynamic analyses has been developed and implemented into the Flowphys Geothermal Flow Assurance software suite. The solver accounts for bending, axial tension/compression, and torsion. It calculates displacement, velocity, and acceleration for 6 Degrees-of-Freedom at every node along the whole drill string. To take into account the effects of the surrounding fluid but still allow for fast calculations, added mass and added damping is used. These can be calculated by two-way coupled fluid-structure interaction (FSI) analyses that includes CFD with viscous fluids. In this report, we use added mass and added damping calculated in previous work [7] where our Flowphys CFD/FSI Arbitrary Lagrangian-Eulerian (ALE) software was used to calculate Navier-Stokes equations around a circular cylinder oscillating inside an annulus. Combined with the fluid, thermodynamic, and heat transfer FEM solvers in this suite, it enables multi-physics simulations of drill string operations under realistic operational conditions.

The fundamentals of the new solver have been described, and a detailed discussion on added mass and added damping is provided. Examples and analytical test cases for validation of both static and dynamic analyses are also shown.

The Flowphys software suite, with its combination of structural dynamics, fluid flow, thermodynamics, and heat transfer solvers forms a Drill String Physics Simulator that forms the fundament for the Drill Monitor in Task 7.3.

6. REFERENCES

1. P. Kjellgren, C.B. Jenssen, H. Yu, T. Peng, GeoDrill deliverable report D7.1 ”Geothermal Well Flow Assurance Simulator”, Jan. 2021
2. PHREEQC Ver. 3; “A computer Program for Speciation, Batch-Reaction, One-Dimensional Transport, and Inverse Geochemical Calculations”, https://wwwbrr.cr.usgs.gov/projects/GWC_coupled/phreeqc/
3. Gert Hedner, ”Formelsamling I Hållfasthetslära”, KTH, Stockholm, 1986
4. R.D. Cook, D.S. Malkus, M.E. Plesha, “Concepts and Applications of Finite Element Analysis”, 3rd Edition, Wiley, 1989
5. W.T. Thomson, “Theory of Vibration”, 3rd Edition, Unwin Hyman, 1988
6. P. Kjellgren, C.B. Jenssen, T. Peng, GeoDrill deliverable report D4.3 ”Design and simulation of fluidic hammer”, April 2020
7. P. Kjellgren & J. Hyvarinen, “An arbitrary Lagrangian-Eulerian finite element method”, Computational Mechanics,21:81-90, 1998
8. S.S. Chen, “Flow-induced vibration of circular cylindrical structures”, Hemisphere, 1987